ACS APPLIED MATERIALS & INTERFACES

Research Article

www.acsami.org

Pd Clusters Supported on Amorphous, Low-Porosity Carbon Spheres for Hydrogen Production from Formic Acid

Dmitri A. Bulushev,*[,†,‡,⊥] Lyubov G. Bulusheva,[§,⊥] Sergey Beloshapkin,[∥] Thomas O'Connor,[†,∥] Alexander V. Okotrub,[§,⊥] and Kevin M. Ryan[†,∥]

[†]Chemical & Environmental Sciences Department, University of Limerick, Limerick, Ireland

[‡]Boreskov Institute of Catalysis, SB RAS, Novosibirsk 630090, Russia

[§]Nikolaev Institute of Inorganic Chemistry, SB RAS, Novosibirsk 630090, Russia

[⊥]Novosibirsk State University, Novosibirsk 630090, Russia

[∥]Materials & Surface Science Institute, University of Limerick, Limerick, Ireland

Supporting Information

ABSTRACT: Amorphous, low-porosity carbon spheres on the order of a few micrometers in size were prepared by carbonization of squalane ($C_{30}H_{62}$) in supercritical CO_2 at 823 K. The spheres were characterized and used as catalysts' supports for Pd. Near-edge X-ray absorption fine structure studies of the spheres revealed sp^2 and sp^3 hybridized carbon. To activate carbons for interaction with a metal precursor, often oxidative treatment of a support is needed. We showed that boiling of the obtained spheres in 28 wt % HNO_3 did not affect the shape and bulk structure of the spheres, but led to creation of a considerable amount of surface oxygen-containing functional groups and increase of the content of sp^2 hybridized carbon on the surface. This carbon was seen by scanning transmission electron microscopy in the form of waving graphene flakes. The H/C atomic ratio in the spheres was relatively high (0.4) and did not change with the HNO_3 treatment. Palladium was deposited by impregnation with Pd acetate followed by reduction in H_2. This gave uniform Pd clusters with a size of 2−4 nm. The Pd supported on the original C spheres showed 2−3 times higher catalytic activity in vapor phase formic acid decomposition and higher selectivity for H_2 formation (98−99%) than those for the catalyst based on the HNO_3 treated spheres. Using of such low-porosity spheres as a catalyst support should prevent mass transfer limitations for fast catalytic reactions.

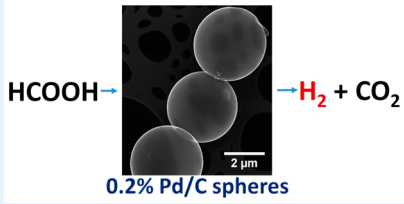

KEYWORDS: *carbon spheres, formic acid, hydrogen production, functional groups, Pd acetate*

INTRODUCTION

The porous structure of catalysts' supports is important for catalytic applications providing an access of reactants to supported metal nanoparticles and desorption of products. Traditionally, activated carbons containing micropores are used as catalysts' supports for noble metal clusters. However, the presence of micropores may lead to deteriorated properties of the catalysts complicating molecular transport or even encapsulating metal clusters.[1] Another reason for deteriorated properties of carbon supported metallic catalysts can be related to nonuniform particle size distributions. The presence of big metal particles decreases the catalytic surface area and amount of active metal surface sites. The deposition of metal precursors can be enhanced on the external surface of the support particle, leading to the formation of bigger metallic particles as compared to those that are formed on the internal surface of the support.

Consequently, a greater understanding of the formation of metal nanoparticles on nonporous and low-porosity carbon supports is of considerable interest. This can be attempted by utilization of carbon spheres with a micrometer or even smaller size. However, the low porosity support should have sufficient concentration of surface anchoring sites for a metal containing precursor to provide the stabilization of metal clusters and to prevent their sintering. Uniform sized carbon microspheres attract increasing attention of researchers not only as catalysts supports, but also as lubricants, precursors for new materials and composites for electrochemical and energy storage applications.[2,3]

Serp et al.[4] used a chemical vapor deposition of a Pt organic precursor to form metallic clusters over low surface area (0.1−0.3 μm) carbon spheres catalytically grown from a CH_4/H_2 mixture at 1373 K. The deposition of Pt on such spheres was possible only after the treatment of the spheres by HNO_3. No catalytic tests of this material were performed in this work and neither the concentration of Pt was determined. Recently, Mondal et al.[5] studied hydrogenation of ethylene over Pd catalysts supported on core−shell carbon spheres (0.5−1 μm) prepared from acetylene at 1073 K. They discovered a higher activity of Pd on the spheres treated with a H_2SO_4/HNO_3 mixture and related this to observed higher dispersion of Pd on the treated supports.

Received: February 3, 2015
Accepted: April 7, 2015
Published: April 7, 2015

DOI: 10.1021/acsami.5b00983
ACS Appl. Mater. Interfaces 2015, 7, 8719−8726

The catalytic formic acid decomposition reaction is widely studied, as formic acid can be used for hydrogen storage[6] or as a hydrogen donor instead of molecular hydrogen for some hydrogenation reactions.[7] Moreover, this acid can be obtained from renewable biomass cellulose by hydrolysis[8] or oxidation.[9,10] Hence, creation of catalysts very selective to the decomposition of formic acid to hydrogen under mild conditions is important. Several research groups have shown that Pd based catalysts are among the best catalysts for this reaction.[11−15] Carbon based materials are mainly used as catalysts supports, as they possess high surface areas, high inertness to the reaction medium and sufficient interaction with noble metal clusters preventing sintering. It is not clear now whether oxygen functional groups created on carbon supports by oxidation in nitric acid or other oxidants can improve or worsen the performance of catalysts in the hydrogen production from formic acid decomposition. High performance of the catalysts can be achieved if the catalyst is in the form of uniform metal clusters of a few nm in size and the reaction is free from mass transport problems.

The temperatures normally used to synthesize carbon spheres (higher than 973 K) can lead to graphitization of these materials.[2−4,16−18] Wu et al.[17] showed that carbon spheres of 0.2−0.5 μm size prepared from acetylene at 1273 K consist of heavily distorted graphene layers. Recently, we have reported that low-porosity uniform amorphous carbon spheres (0.3−1.5 μm) with superhydrophobic properties can be synthesized by pyrolysis of squalane ($C_{30}H_{62}$) in supercritical CO_2 at temperatures as low as 773 K.[19] In the present paper, we study further the structure and composition of these original spheres and the spheres treated by HNO_3, prior to using them as catalysts' supports for Pd clusters (2−4 nm) to produce hydrogen effectively from vapor phase formic acid decomposition at low temperatures (<423 K).

EXPERIMENTAL SECTION

Materials. The details for synthesis of carbon spheres can be found elsewhere.[19] Experiments were conducted using liquid carbon dioxide from BOC (99.85%). A Teledyne model 260D computer controlled syringe pump was used to pressurize the system. All experiments were conducted using a three-zone heating furnace. Colloidal carbon spheres with an average size of 3 μm were synthesized by carbonization of squalane (99%, Sigma-Aldrich) at 823 K and supercritical CO_2 pressures of 35 MPa. In a typical synthesis, a reaction cell (120 mL, 316 stainless steel) was loaded with 1 mL of squalane in a glovebox environment. The cell was sealed under nitrogen before removal and connection to a supercritical pump using stainless steel tubing. Liquid CO_2 was then pumped into the reaction cell and the pressure was increased above its critical point to 35 MPa. The furnace was preheated to 838 K prior to inserting the reaction cell. All parameters were kept constant for the preceding period of 45 min, after which the furnace was opened and cooled to room temperature before venting of CO_2. A black powder containing the yield of amorphous carbon spheres was observed upon completion of a synthesis and could be collected from the reaction vessel using portions of toluene (original spheres). Some of the sphere product was boiled in 28 wt % HNO_3 for 2 h, washed in distilled water until neutral pH of solution and dried overnight in air at 378 K (HNO_3 treated spheres).

Pd was deposited on the spheres using incipient wetness impregnation. For this, Pd acetate (Aldrich) was dissolved in acetone in an amount to provide the metal content of 0.2 wt %. After the complete consumption of the solution by the support, the material was dried overnight at 353 K in air.

Characterization Methods. The content of C, H and N elements in the samples was provided by an Elementar "Vario EL Cube" system; the oxygen content was determined by difference. The Brunauer−Emmet−Teller (BET) surface area of the spheres was measured by nitrogen adsorption using a Micromeritics Gemini system. Before the measurements, the samples were treated in a flow of nitrogen at 473 K for 2 h. Infrared (IR) spectra were obtained on a PerkinElmer Spectrum 100 unit with an attenuated total reflectance (ATR) accessory. Raman spectra were recorded on a Dilor XY Labram spectrometer equipped with a 20 mW ArHe laser and a Peltier cooled CCD detector.

Near-edge X-ray absorption fine structure (NEXAFS) spectra were measured at the Berliner Elektronenspeicherring für Synchrotronstrahlung (BESSY) using radiation from the Russian−German beamline. The C K-edge spectra were acquired in the total-electron yield (TEY) and Auger-electron yield (AEY) modes with a typical probing depth of about 10 nm and less than 1 nm, respectively. The spectra were normalized to the primary photon current from a gold-covered grid recorded simultaneously.

The structure of the samples was analyzed using scanning transmission electron microscopy (STEM) on a JEOL JEM-2100F microscope. For STEM imaging the signal from the backscattered electron image (BEI) detector in a secondary electron detection mode was used. X-ray photoelectron spectroscopy (XPS) measurements were performed on a Kratos AXIS Ultra DLD spectrometer using monochromatic Al Kα radiation of energy 1486.6 eV. C 1s line at 284.8 eV was taken for reference energy calibration. It is known that metallic Pd is covered by a thin oxide layer in ambient air. To remove this, the already reduced Pd catalysts supported on carbon spheres were reduced additionally at 33 Pa of pure hydrogen at 573 K for 30 min in the preparation chamber of the XPS unit and transferred to the measurement chamber in ultrahigh vacuum conditions (10^{-6} Pa) without contact with air.

Catalytic Measurements. For catalytic experiments, 0.0035 g of the Pd catalyst supported on carbon spheres was placed in a quartz fixed bed reactor of 4 mm internal diameter. The sample was reduced in an 1 vol % H_2/Ar mixture at 573 K for 1 h and cooled in He to the reaction temperature. An equivalent reductive pretreatment of some catalysts was performed before their transfer in air to different equipment for characterization.

Formic acid was introduced into an evaporation volume using a syringe-pump (Sage); the content of formic acid in the created reaction mixture was 2 vol %. Helium was used as a carrier gas. All gases were provided by BOC Gases and were introduced to the system via mass-flow controllers. The reactants and products were analyzed by a gas chromatograph (HP-5890) fitted with a Porapak-Q column and a thermal conductivity detector. The turnover frequency values (TOF) were determined as the ratio of the rate of CO and CO_2 formation from formic acid to the number of surface Pd sites, evaluated from TEM determinations of the mean Pd particle size.

RESULTS

Carbon Spheres. STEM analysis showed that the HNO_3 treated spheres have uniform size of 3 μm (Figure 1a) being indistinguishable from that of the original spheres (Figure 1b). The spheres are partially transparent to the electron beam, indicating their low density and absence of interior texture. Similarly to the as-synthesized material,[19] the treated spheres are assembled, probably, by van der Waals forces.[3] An attempt to get an electron diffraction pattern of the spheres in the TEM unit confirmed that the HNO_3 treated spheres as well as the original ones[19] are amorphous, as they do not provide any diffraction pattern. We postulate that the spheres consist of disordered graphene fragments of different sizes. This is supported by Raman spectroscopy, which reveals two major bands located at 1596 and 1350 cm^{-1} (Figure S1 of the Supporting Information) in the 1200−1700 cm^{-1} region corresponding to G and D bands in graphitic materials.[20] The former band is activated by tangential bond vibrations in

DOI: 10.1021/acsami.5b00983
ACS Appl. Mater. Interfaces 2015, 7, 8719−8726

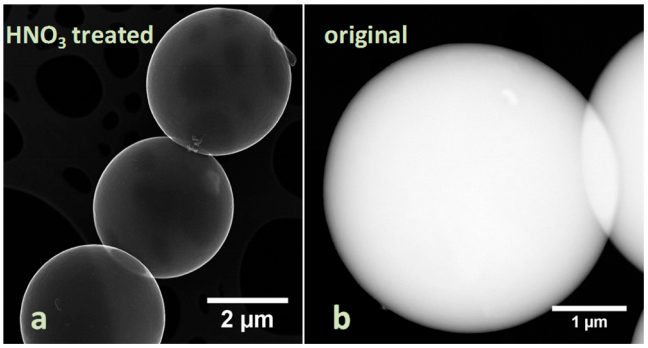

Figure 1. STEM image of the (a) HNO_3 treated and (b) original carbon spheres.

sp^2 carbon network while the latter band has a disorder-induced character. The spectra of the original and HNO_3 treated spheres have a high intensity ratio of the D band to the G band (equal to 0.9) denoting the presence of a considerable amount of lattice edges and defects in the studied samples.

Generally, both the Raman spectroscopy and microscopy studies indicate that the HNO_3 treatment does not destroy the structure of the spheres. However, as we will show later the treatment changes the surface chemical composition of the spheres. The ratio of the amount of surface atoms to the total amount of atoms in the studied materials is small. Hence, the effect of the HNO_3 treatment is not seen by Raman spectroscopy demonstrating mainly the bulk of these spheres.

The difference between the surface and the bulk of the spheres is clear when the NEXAFS C K-edge spectra measured in the AEY and TEY modes are compared (Figure 2). The spectra have two major peaks at ~285.2 and around ~292.5 eV assigned to the 1s→π^* and 1s→σ^* electron transitions. As compared to the C K-edge spectrum of graphite (Figure S2 of the Supporting Information), the π^* and σ^* resonances are significantly broadened, evidencing poor atomic ordering in the spheres. A peak in the spectra at ~287.8 eV correlates to

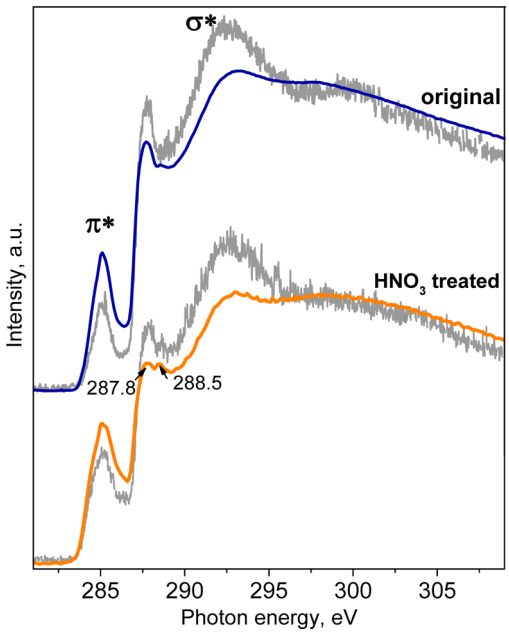

Figure 2. NEXAFS C K-edge spectra of the original and HNO_3 treated spheres measured in AEY (gray) and TEY (color) modes.

functionalization of carbon. The higher intensity of this peak in the spectra recorded in the AEY mode (Figure 2) is due to a larger content of functional groups on the surface of the spheres. After the HNO_3 treatment, the C K-edge spectrum shows an increase in the relative intensity of the π^* resonance and a decrease in the intensity and splitting of the peak located between the π^* and σ^* resonances. Previously, similar changes have been observed in the NEXAFS spectra after boiling of graphite oxide in concentrated H_2SO_4 and H_3PO_4 acids.[21] The enhancement of the π^* resonance could be related to removal of amorphous carbon species from the surface by the acid. Graphene layers responsible for the π^* resonance become exposed to the surface, as they are considerably less reactive.

The change in the shape of the peak at about 288 eV is attributed to modification of chemical composition of the spheres. Two peaks at 287.8 and 288.5 eV, which are resolved in the C K-edge spectrum of the HNO_3 treated spheres, can be attributed to epoxy (C−O−C) and carboxyl (COOH) groups, respectively.[22] It is known that C−H bonds can contribute to the former peak[24] and we cannot reject the presence of such species in our samples as the content of hydrogen was relatively high (Table 1). However, the NEXAFS studies showed that the

Table 1. Bulk Elemental Composition of the Carbon Spheres (at. %)

	C	H	N	O[a]	H/C atomic ratio
original	71.7	27.8	0	0.5	0.39
HNO_3 treated	65.3	24.7	1.5	8.5	0.38

[a]Determined as a difference from 100%.

species responsible for the 287.8 eV line are located mainly on the surface (Figure 2) and the treatment in HNO_3 leads to a considerable decrease of the intensity of this line, but the change in the total content of hydrogen is negligible (Table 1). Thus, we can attribute the line at 287.8 eV mainly to epoxy groups and the drop in the relative intensity of this peak as the result of boiling in HNO_3 could be due to partial oxidation of epoxy groups to carboxyl groups and CO, CO_2.

The change in the composition of the spheres after the HNO_3 treatment was confirmed by elemental analysis of the original and treated materials. The data listed in Table 1 indicate that the spheres contain a considerable amount of hydrogen corresponding to an H/C atomic ratio of about 0.4. This value is typical for amorphous carbon films.[23] The treatment with HNO_3 leads to a considerable increase in the concentration of oxygen by a factor of 17 as well as to the formation of some nitrogen containing species.

In accordance, XPS analysis of the C 1s (Figure S3 of the Supporting Information) and O 1s (Figure S4 of the Supporting Information) lines for the spheres indicated a considerable increase in the content of oxygen functional groups on the surface. The surface content of oxygen in both investigated materials was higher as compared to the bulk content (Table 1), indicating that the oxygen is located mainly on the surface. For the original spheres, the oxygen containing functional groups can be formed by interaction of wet ambient air with surface carbon species of unsaturated valences on removing the spheres from the reaction cell.

XPS analysis of the treated spheres showed the presence of a peak at 406.0 eV (Figure S5 of the Supporting Information) in the N 1s region, which is typical for nitro groups ($-NO_2$).[24] The presence of these groups indicates that boiling of the

DOI: 10.1021/acsami.5b00983
ACS Appl. Mater. Interfaces 2015, 7, 8719−8726

spheres in HNO_3 leads to nitration of some carbon species in the sample. These groups contribute to the shape of the C 1s and O 1s lines as well as the oxygen content in the sample. The C 1s line was fitted with three components at 284.8, 286.3–286.5 and 289.1–289.3 eV (Figure S3 of the Supporting Information), which are assigned to sp^2/sp^3 carbon, C–OR/C–OH groups and carboxylic species, respectively. The O 1s line for the original carbon spheres was fitted with two components at 532.4 and 534.1 eV (Figure S4 of the Supporting Information), which correspond to ether-like C–O groups and carboxylic/phenolic species, respectively. The HNO_3 treatment led to the appearance of the additional O 1s line at 533.4 eV, which is related to the formation of nitro or some carboxylic groups.[25]

The development of the nitro and carboxyl groups with the acidic treatment is further supported by ATR-IR spectra (Figure S6 of the Supporting Information). Actually, two new bands appear at 1522 and 1322 cm^{-1} due to vibrations in nitro groups[26] and a band at 1712 cm^{-1} assigned to C=O vibration in carboxyl groups[27] becomes considerably stronger. A broad band appears also at 3430 cm^{-1} and corresponds to hydrogen bonded hydroxyl groups. These could be present in the form of the mentioned carboxyl and/or phenolic groups. Generally, the presence of the hydrogen bonded hydroxyl groups indicates that the carbon spheres become hydrophilic.

The BET surface area measurement of the original sample showed a very low value of 2.8 $m^2\ g^{-1}$. This value is about two times higher than the geometric surface area of these spheres calculated accepting a density of 1.8 g cm^{-3}.[28] This relatively small difference between the geometric and BET surface areas indicates that the studied carbon spheres are low-porosity materials in accordance with our earlier consideration.[19]

Summarizing, the obtained amorphous and low-porosity spheres have a size of 3 μm. They can be assigned to a type of solid spheres[3] containing a considerable amount of hydrogen. The HNO_3 treatment does not destroy the bulk structure of the spheres, but changes the surface composition, creating more sp^2 carbon on the surface and different oxygen containing groups (carboxylic, phenolic, nitro), which make the surface hydrophilic.

Pd on Carbon Spheres. XPS spectra of the Pd 3d region of the spheres with deposited Pd acetate are shown in Figure 3. Pd on the HNO_3 treated spheres is presented in a single state

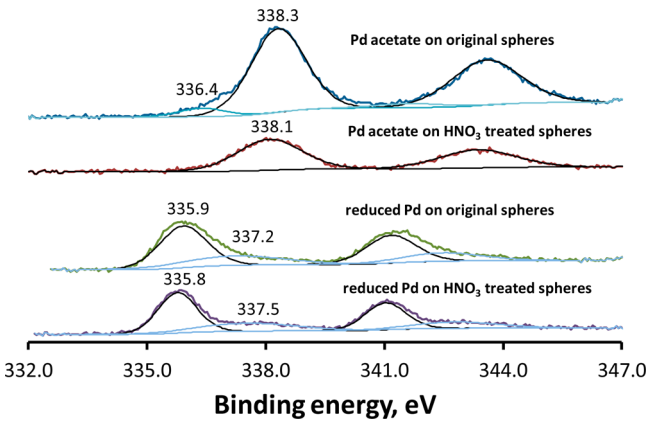

Figure 3. XPS spectra of the Pd 3d region for the 0.2 wt % Pd catalysts supported on the original and HNO_3 treated carbon spheres before and after reduction in the catalytic reactor and XPS unit.

with the Pd $3d_{5/2}$ binding energy of 338.1 eV. This line corresponds to Pd^{2+} in adsorbed Pd acetate-like species as it was previously observed for pure Pd acetate.[29] The corresponding C 1s line, typical for acetate, was also observed at approximately 289 eV (not shown). The position for the Pd acetate-like species supported on the original spheres is slightly shifted to a higher binding energy of 338.3 eV. At the same time, another weak line of Pd $3d_{5/2}$ at 336.4 eV is also observed for this sample. The content of this Pd state is small and corresponds only to 8% from the total content of Pd in the sample. This line is normally assigned to Pd^{2+} in PdO_x species.[30,31] However, Pd clusters with a few atoms may also provide a Pd $3d_{5/2}$ line in the same region.[32,33] It should be mentioned that the presence of two Pd species after acetate deposition on the original spheres as compared to the HNO_3 treated spheres could affect the final particle size distribution in the reduced catalysts.

XPS study showed that the carbon spheres do not reduce Pd acetate during its deposition and drying at 353 K. It can also be important that the intensity of the Pd peak in the original spheres is 3 times higher than that in the HNO_3 treated spheres corresponding to 1.3 and 0.44 at. %, respectively. This may indicate that Pd acetate being supported on the original spheres is more highly dispersed while that adsorbed on the HNO_3 treated spheres forms bigger Pd acetate particles or is located between surface graphene layers leading to shielding of its signal.

The values of the total surface content of Pd determined by XPS after the H_2 reduction of the samples supported on the original and HNO_3 treated samples become close to each other (0.84 and 0.62, respectively), but still some difference is observed (Table 2). The electronic state of Pd for the reduced

Table 2. Surface Atomic Concentrations of Elements in the Reduced Pd Catalysts on Carbon Spheres Determined by XPS (at. %)

	C	O	N	Pd
Pd catalyst on the original spheres	92.55	6.61	0	0.84
Pd catalyst on the HNO_3 treated spheres	85.28	10.4	3.69	0.62

samples is different from that in the unreduced samples with Pd acetate observed after Pd deposition and drying (Figure 3). The spectra of Pd after reduction demonstrate a metallic Pd state (Pd^0) with the Pd $3d_{5/2}$ line at about 335.8 eV as well as an oxidized Pd state (Pd^{2+}) with the $3d_{5/2}$ position at about 337.2–337.5 eV.[31,34] The binding energy for the metallic state of Pd is shifted with respect to that in the bulk Pd (335.0–335.2 eV).[31−34] This was attributed to a very small size of metallic clusters. At the same time, the second Pd state is different from that observed for the Pd acetate supported on the spheres (338.1–338.3 eV, Figure 3). The content of the oxidized state in the reduced samples is about 30%. The incomplete reduction of Pd on the spheres is probably related to very small oxidized particles and/or strong interaction of some Pd^{2+} species with specific sites on the support's surface.

STEM images of the Pd catalysts supported on spheres after the reduction/reaction are shown in Figure 4. The surface of the original sample looks quite uniform, but is not flat, as it consists of small pits and hills. Graphene flakes are not seen as, probably, they are covered by amorphous carbon. In contrast, the surface of the HNO_3 treated spheres is less uniform (Figure 4b). Small regions with pits and hills similar to those for the

DOI: 10.1021/acsami.5b00983
ACS Appl. Mater. Interfaces 2015, 7, 8719–8726

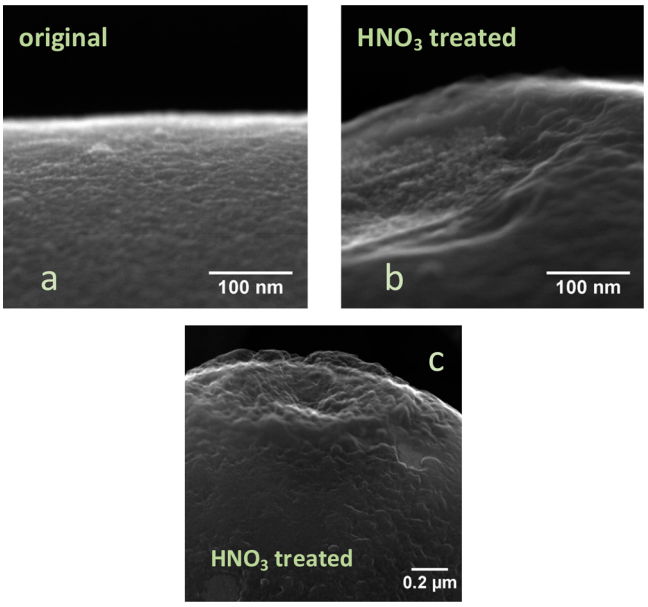

Figure 4. STEM images of the surface part of the 0.2 wt % Pd catalysts supported on the (a) original and (b,c) HNO_3 treated carbon spheres after the reaction (Pd clusters are not seen).

original spheres (Figure 4a) are still visible. However, relatively big pieces of waving graphene flakes are mainly seen (Figure 4b,c). This is in line with the NEXAFS C K-edge data showing the presence of a higher content of sp^2 hybridized carbon in the surface layer of the HNO_3 treated spheres than in the original spheres. Deshmukh et al.[3] indicate that such waving is provided by replacement of C6 rings by C5 and C7 rings in the structure of flakes. This replacement is important and may lead to different chemical properties of the surfaces as compared to graphite or graphene.

STEM images of the Pd samples after the reduction/reaction demonstrating Pd clusters over the both supports are shown in Figure 5. The mean Pd particle size on the HNO_3 treated spheres is about 3.1 nm whereas that on the original spheres is slightly higher, 3.7 nm. It is seen again that the carbon surface

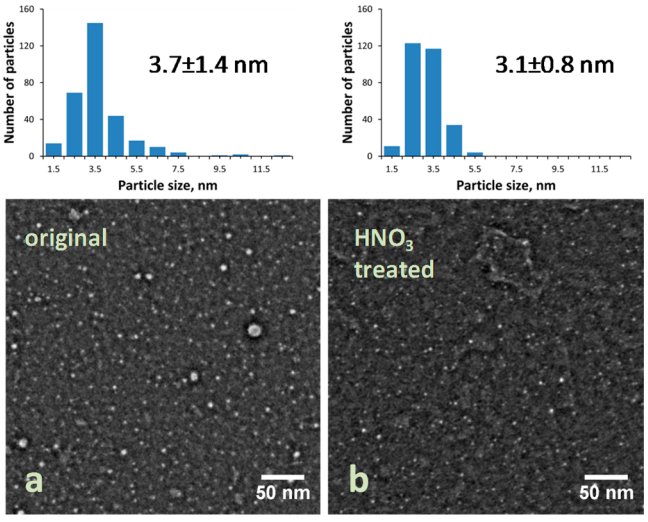

Figure 5. STEM images and particle size distributions for the 0.2 wt % Pd catalysts supported on the (a) original and (b) HNO_3 treated carbon spheres after the reaction.

in the HNO_3 treated sample looks inhomogeneous as compared to the original sample, as carbon pieces of more than 25 nm in size are seen. In spite of this, Pd clusters are distributed homogeneously over the both supports. Meanwhile, the HNO_3 treated spheres provide more uniform Pd particle size distribution and they do not contain the particles with a size of bigger than 5.5 nm. The presence of a tail of particles bigger than 5.5 nm for the sample supported on the original spheres is probably related to the initial presence of two types of Pd^{2+} species with Pd $3d_{5/2}$ at 336.4 and 338.3 eV observed by XPS (Figure 3) in this sample. During the reduction, the growth of Pd clusters on two different nuclei present after the Pd acetate deposition may affect the shape of the Pd particles size distribution.

Catalytic Properties. Conversions of formic acid and selectivities to hydrogen production on the Pd catalysts supported on carbon spheres are shown in Figure 6 as a

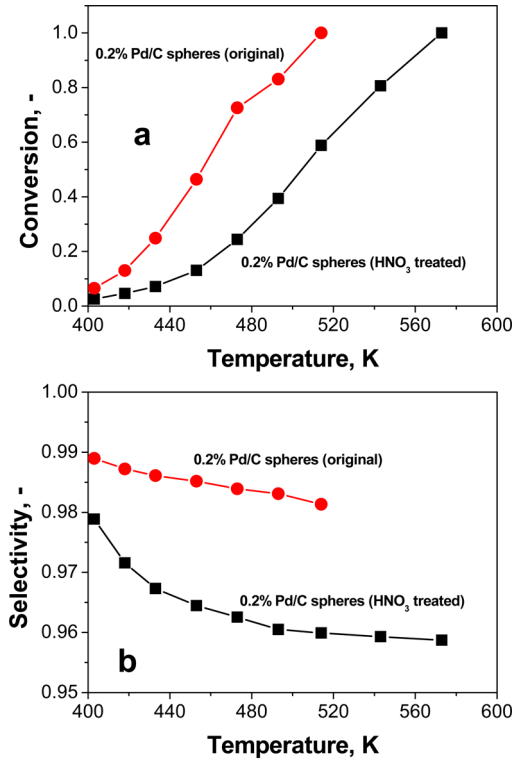

Figure 6. Conversion (a) and hydrogen selectivity (b) for the formic acid decomposition as functions of the temperature for the 0.2 wt % Pd/carbon spheres.

function of temperature. It is seen that the conversion at low temperatures is 2−3 times higher on the catalyst based on the original spheres. The selectivity for this catalyst is in the range of 98−99%. The selectivity for the catalyst based on the HNO_3 treated spheres is lower, 96−98%. The turnover frequency (TOF) values were calculated and are shown in the Arrhenius plot (Figure S8 of the Supporting Information). The TOFs are also noticeably higher for the catalyst based on the original spheres. The apparent activation energies for the formic acid decomposition for the catalysts based on the original and HNO_3 treated spheres are different and correspond to 65 and 50 kJ mol^{-1}, respectively. Hence, in spite of the fact that the activation energy is higher for the catalyst based on the original

DOI: 10.1021/acsami.5b00983
ACS Appl. Mater. Interfaces 2015, 7, 8719−8726

spheres, its performance in the reaction (activity and selectivity) is better.

Earlier, we reported the catalytic data for a commercial 1 wt % Pd catalyst supported on activated carbon (Sigma-Aldrich).[11] This sample had a quite similar Pd mean particle size (3.6 nm) as compared to that for Pd on the studied carbon spheres. The selectivity and apparent activation energy values for this catalyst were also close to the values for the Pd on the original spheres and corresponded to 98−99% and 65 kJ mol^{-1}, respectively. Therefore, the catalysts supported on the low-porosity spheres show comparable catalytic properties to the commercial Pd catalyst supported on activated carbon.

DISCUSSION

Carbon Spheres. The results of the performed research confirmed that carbon spheres synthesized from squalane in supercritical CO_2 are uniform in size, amorphous and have low porosity. We demonstrate that the spheres contain sp^2 carbon mainly in the bulk and a lot of sp^3 carbon probably partially involved in the formation of C−H bonds. This is not surprising as the saturated hydrocarbon ($C_{30}H_{62}$) with high content of hydrogen was used for synthesis at a relatively low temperature (823 K).

Our STEM (Figure 4) and C K-edge NEXAFS (Figure 2) data indicate that the HNO_3 treatment affects the surface of the spheres providing its enrichment with graphene flakes. The difference between the original and HNO_3 treated spheres can be explained by removal of a thin amorphous layer from the flakes surface keeping the relatively inert graphene flakes intact. However, the bulk of the spheres is still amorphous as HNO_3 has access only to the surface. In accordance with multiple literature data, this treatment leads to creation of a considerable amount of oxygen functional groups including phenolic and carboxylic, which make the surface hydrophilic. Additionally, the existing oxygen containing epoxy groups can be further oxidized to carboxylic groups. The fact that more oxygen groups are formed indicates that the surface of an average graphene flake is still very small and this provides the presence of a considerable amount of carbon open edges with dangling bonds.[2] This carbon can be further oxidized by HNO_3.

Deposition of Pd on Carbon Spheres. In spite of the superhydrophobic properties of the original carbon spheres,[19] they interact with Pd acetate forming adsorbed Pd acetate-like species. The surface of the HNO_3 treated spheres is less uniform than that of the original spheres and includes two regions: the region of small pits and hills typical for the original spheres and a main region of waving graphene flakes. The uniformity of the original spheres could be a reason of a few times higher surface concentration of deposited Pd acetate in that case demonstrated by XPS (Figure 3). The existence of interaction of Pd acetate with the original support shows that the necessary support anchoring sites are already present in sufficient concentration. These can be epoxy groups observed by NEXAFS. The reduction of the catalyst leads to a decrease of the surface Pd concentration for this material indicating sintering and growth of metallic particles.

The interaction of Pd acetate with carbon spheres differs from interaction of some other Pd precursors with carbons,[36] as carbon spheres themselves were not able to reduce Pd^{2+} in Pd acetate into metallic state at the used conditions. In accordance, Kondrat et al.[37] showed in a gravimetric study that Pd acetate thermally decomposes in an inert atmosphere at relatively high temperatures (higher than 463 K). The resistance of Pd acetate to thermal treatment probably determines the uniform metal particle size distribution observed after the reduction.

In contrast to the original spheres, the HNO_3 treated spheres provide a lower dispersion of Pd acetate over the surface. Some of Pd acetate can be inserted between the graphene layers. The initial consumption of Pd acetate in this case could be tentatively assigned to its interaction with OH groups in phenolic or carboxylic groups like it was presented, for example, by Santacesaria et al.:[38]

$$Pd(CH_3COO)_2 + \|-OH \rightarrow \|-OPd(CH_3COO) + CH_3COOH \quad (1)$$

The followed reduction of the Pd acetate species at increased temperatures leads to an increase of the surface concentration of Pd for this sample, indicating removal of the acetate shell and formation of metallic nanoparticles. The formed oxygen containing groups can facilitate the surface diffusion of metallic Pd clusters providing their optimized distribution over the surface forming 2−4 nm sized clusters. In accordance, Kondrat et al.[37] have shown that even dry physical grinding of Pd acetate with high surface area activated carbon followed by heating in an inert gas led to relatively low Pd particle sizes (2−4 nm). However, some bigger Pd crystals (20 nm) were also formed.

Serp et al.[4] demonstrated the necessity of the HNO_3 treatment of their carbon spheres prepared at 1373 K for interaction with a Pt containing organic precursor. Similarly, we showed earlier the absence of interaction of $[Au(ethylenediamine)_2]Cl_3$ complex with porous carbon microfibers, which did not contain oxygen containing functional groups after pretreatment in helium at 1273 K.[39] In contrast, the amorphous carbon spheres synthesized in this work at a low temperature (823 K) demonstrated excellent interaction with Pd acetate. The difference between the results of these works can indicate that extended graphitization of the carbon samples at high temperatures accompanied by removal of functional groups and carbon dangling bonds leads to a decrease of the concentration of anchoring sites for interaction with a precursor.

Catalytic Properties of Pd on Carbon Spheres. Interestingly, the HNO_3 treatment of the carbon spheres negatively affects the catalytic activity as well as the selectivity for hydrogen production from the formic acid decomposition (Figure 6). Hence, the HNO_3 treatment is not needed, as quite uniform Pd particles of, probably, optimal sizes (2−4 nm) for the formic acid decomposition[15,40] are formed after the reduction of adsorbed Pd acetate on the original spheres. Earlier, we demonstrated a similar effect of the HNO_3 treatment on carbon microfibers in CO oxidation over supported Au.[39] This was assigned to different metal particle sizes formed on the original and HNO_3 treated carbon microfibers. In contrast, Mondal et al.[5] have shown that Pd on treated with acids carbon spheres with crystalline shell is more active in hydrogenation of ethylene than Pd on original carbon spheres. They explained the result also by a particle size effect as the particle size distributions and mean sizes were different. In the present work, the mean Pd particle sizes were equal to 3.7 and 3.1 nm on the original and HNO_3 treated spheres, respectively. Meanwhile, the small negative effect of the HNO_3 treatment was still observed. XPS data indicate that there is some difference in the surface concentration of Pd in the samples (Table 2). Some Pd can be not accessible by formic acid being located between the surface graphene layers in the HNO_3 treated samples. The differences can be also related to

DOI: 10.1021/acsami.5b00983
ACS Appl. Mater. Interfaces 2015, 7, 8719−8726

the structure of Pd clusters and/or effect of hydrophilicity of the support surface on the conversion of formic acid. Gosselink et al.[41] reported recently such effect of support's polarity for activation of stearic acid ($C_{18}H_{36}O_2$) in deoxygenation reactions over Pd nanoparticles. It is important, however, that the catalytic properties of the Pd supported on spheres (selectivity, activation energies) were quite close to the properties of the commercial Pd catalyst supported on activated carbon implying that the benefit of high accessibility of Pd nanoparticles by reactants can be used, for example, in hydrogenation reactions with formic acid as a hydrogen donor. Further improvement of the catalytic properties can be possible by using bi- or trimetallic[15,42,43] compositions of clusters, doping of the catalysts with alkali metal carbonates/formates[12,31] or applying of nitrogen-doped carbon supports.[44−46]

CONCLUSIONS

Low-porosity, amorphous carbon spheres of uniform 3 μm size prepared from squalane in supercritical CO_2 at a quite low temperature (823 K) were used as catalysts' supports for Pd clusters. Uniformly distributed Pd clusters of 2−4 nm size were prepared on the original and HNO_3 treated spheres by incipient wetness impregnation of Pd acetate in acetone followed by reduction in H_2. The catalyst based on the original spheres showed slightly higher activity and selectivity for production of hydrogen from vapor phase decomposition of formic acid than the catalyst based on the HNO_3 treated spheres. Hence, the HNO_3 treatment was not needed to create an active catalyst. Using of the developed low-porosity spheres as a catalyst support should provide some advantages with respect to microporous activated carbons like the absence of encapsulation of metal particles inside carbon micropores as well as avoiding mass transfer limitations for fast catalytic reactions.

ASSOCIATED CONTENT

Supporting Information

Raman spectra (Figure S1), comparison of the NEXAFS spectra of the original carbon spheres with the spectrum of graphite (Figure S2), XPS spectra (Figures S3−S5 and S7) and ATR-IR spectra of the spheres (Figures S6). This material is available free of charge via the Internet at http://pubs.acs.org.

AUTHOR INFORMATION

Corresponding Author

*D. A. Bulushev. E-mail: dmitri.bulushev@ul.ie.

Notes

The authors declare no competing financial interest.

ACKNOWLEDGMENTS

This publication has emanated from research conducted with the financial support of Science Foundation Ireland under Grant Number 06/CP/E007. K.R. would like to acknowledge Science Foundation Ireland for grants 11-PI-1148 and 06/IN.1/I85 TIDA Feasibility 10. This work is also in part funded by the Irish Government under the Programme for Research in Third-Level Institutions (PRTLI) Cycle 5 and co-funded under the European Regional Development Fund. Additionally, the authors thank the SEED funding of the University of Limerick and highly appreciate the assistance of Alen Horvat and Lijun Jia (University of Limerick).

REFERENCES

(1) Gurrath, M.; Kuretzky, T.; Boehm, H. P.; Okhlopkova, L. B.; Lisitsyn, A. S.; Likholobov, V. A. Palladium Catalysts on Activated Carbon Supports Influence of Reduction Temperature, Origin of the Support and Pretreatments of the Carbon Surface. *Carbon* **2000**, *38*, 1241−1255.

(2) Nieto-Marquez, A.; Romero, R.; Romero, A.; Valverde, J. L. Carbon Nanospheres: Synthesis, Physicochemical Properties and Applications. *J. Mater. Chem.* **2011**, *21*, 1664−1672.

(3) Deshmukh, A. A.; Mhlanga, S. D.; Coville, N. J. Carbon Spheres. *Mater. Sci. Eng., R* **2010**, *70*, 1−28.

(4) Serp, P.; Feurer, R.; Kihn, Y.; Kalck, P.; Faria, J. L.; Figueiredo, J. L. Novel Carbon Supported Material: Highly Dispersed Platinum Particles on Carbon Nanospheres. *J. Mater. Chem.* **2001**, *11*, 1980−1981.

(5) Mondal, K. C.; Cele, L. M.; Witcomb, M. J.; Coville, N. J. Carbon Microsphere Supported Pd Catalysts for the Hydrogenation of Ethylene. *Catal. Commun.* **2008**, *9*, 494−498.

(6) Grasemann, M.; Laurenczy, G. Formic Acid as a Hydrogen Source - Recent Developments and Future Trends. *Energy Environ. Sci.* **2012**, *5*, 8171−8181.

(7) Bulushev, D. A.; Ross, J. R. H. Vapour Phase Hydrogenation of Olefins by Formic Acid over a Pd/C Catalyst. *Catal. Today* **2011**, *163*, 42−46.

(8) Hayes, D. J.; Fitzpatrick, S.; Hayes, M. H. B.; Ross, J. R. H. In *Biorefineries-Industrial Processes and Products*; Kamm, B., Gruber, P. R., Kamm, M., Eds.; Wiley-VCH: Weinheim, 2006; Vol. *1*, pp 139−164.

(9) Li, J.; Ding, D. J.; Deng, L.; Guo, Q. X.; Fu, Y. Catalytic Air Oxidation of Biomass-Derived Carbohydrates to Formic Acid. *ChemSusChem* **2012**, *5*, 1313−1318.

(10) Zhang, J.; Sun, M.; Liu, X.; Han, Y. Catalytic Oxidative Conversion of Cellulosic Biomass to Formic Acid and Acetic Acid with Exceptionally High Yields. *Catal. Today* **2014**, *233*, 77−82.

(11) Bulushev, D. A.; Beloshapkin, S.; Ross, J. R. H. Hydrogen from Formic Acid Decomposition over Pd and Au Catalysts. *Catal. Today* **2010**, *154*, 7−12.

(12) Bulushev, D. A.; Jia, L. J.; Beloshapkin, S.; Ross, J. R. H. Improved Hydrogen Production from Formic Acid on a Pd/C Catalyst Doped by Potassium. *Chem. Commun.* **2012**, *48*, 4184−4186.

(13) Solymosi, F.; Koós, Á.; Liliom, N.; Ugrai, I. Production of CO-Free H_2 from Formic Acid. A Comparative Study of the Catalytic Behavior of Pt Metals on a Carbon Support. *J. Catal.* **2011**, *279*, 213−219.

(14) Hu, C.; Ting, S.-W.; Chan, K.-Y.; Huang, W. Reaction Pathways Derived from DFT for Understanding Catalytic Decomposition of Formic Acid into Hydrogen on Noble Metals. *Int. J. Hydrogen Energy* **2012**, *37*, 15956−15965.

(15) Tedsree, K.; Li, T.; Jones, S.; Chan, C. W. A.; Yu, K. M. K.; Bagot, P. A. J.; Marquis, E. A.; Smith, G. D. W.; Tsang, S. C. E. Hydrogen Production from Formic Acid Decomposition at Room Temperature Using a Ag-Pd Core-Shell Nanocatalyst. *Nat. Nanotechnol.* **2011**, *6*, 302−307.

(16) Nieto-Marquez, A.; Toledano, D.; Sanchez, P.; Romero, A.; Valverde, J. L. Impact of Nitrogen Doping of Carbon Nanospheres on the Nickel-Catalyzed Hydrogenation of Butyronitrile. *J. Catal.* **2010**, *269*, 242−251.

(17) Wu, H. C.; Hong, C. T.; Chiu, H. T.; Li, Y. Y. Continuous Synthesis of Carbon Spheres by a Non-catalyst Vertical Chemical Vapor Deposition. *Diamond Relat. Mater.* **2009**, *18*, 601−605.

(18) Pol, V. G.; Motiei, M.; Gedanken, A.; Calderon-Moreno, J.; Yoshimura, M. Carbon Spherules: Synthesis, Properties and Mechanistic Elucidation. *Carbon* **2004**, *42*, 111−116.

(19) Barrett, C. A.; Singh, A.; Murphy, J. A.; O'Sullivan, C.; Buckley, D. N.; Ryan, K. M. Complete Synthesis of Germanium Nanocrystal Encrusted Carbon Colloids in Supercritical CO_2 and their Superhydrophobic Properties. *Langmuir* **2011**, *27*, 11166−11173.

(20) Pimenta, M. A.; Dresselhaus, G.; Dresselhaus, M. S.; Cançado, L. G.; Jorio, A.; Saito, R. Studying Disorder in Graphite-based Systems by Raman Spectroscopy. *Phys. Chem. Chem. Phys.* **2007**, *9*, 1276−1291.

DOI: 10.1021/acsami.5b00983
ACS Appl. Mater. Interfaces 2015, 7, 8719−8726

(21) Okotrub, A. V.; Yudanov, N. F.; Tur, V. A.; Asanov, I. P.; Shubin, Y. V.; Vyalikh, D. V.; Bulusheva, L. G. Perforation of Graphite in Boiling Mineral Acid. *Phys. Status Solidi B* **2012**, *249*, 2620−2624.
(22) Hunt, A.; Dikin, D. A.; Kurmaev, E. Z.; Boyko, T. D.; Bazylewski, P.; Chang, G. S.; Moewes, A. Epoxide Speculation and Functional Group Distribution in Graphene Oxide Paper-like Materials. *Adv. Funct. Mater.* **2012**, *22*, 3950−3957.
(23) Chen, G. Y.; Stolojan, V.; Silva, S. R. P.; Herman, H.; Haq, S. Carbon Spheres Generated in "Dusty Plasmas". *Carbon* **2005**, *43*, 704−708.
(24) Zhang, G. X.; Sun, S. H.; Yang, D. Q.; Dodelet, J. P.; Sacher, E. The Surface Analytical Characterization of Carbon Fibers Functionalized by H_2SO_4/HNO_3 Treatment. *Carbon* **2008**, *46*, 196−205.
(25) Arrigo, R.; Havecker, M.; Wrabetz, S.; Blume, R.; Lerch, M.; McGregor, J.; Parrot, E. P. J.; Zeitler, J. A.; Gladden, L. F.; Knop-Gericke, A.; Schlogl, R.; Su, D. S. Tuning the Acid Base Properties of Nanocarbons by Functionalization via Amination. *J. Am. Chem. Soc.* **2010**, *132*, 9616−9630.
(26) Muckenhuber, H.; Grothe, H. A DRIFTS Study of the Heterogeneous Reaction of NO_2 with Carbonaceous Materials at Elevated Temperature. *Carbon* **2007**, *45*, 321−329.
(27) Subrahmanyam, C.; Bulushev, D. A.; Kiwi-Minsker, L. Dynamic Behaviour of Activated Carbon Catalysts During Ozone Decomposition at Room Temperature. *Appl. Catal., B* **2005**, *61*, 98−106.
(28) Hammond, C. R. In *CRC Handbook of Chemistry and Physics*; 86 ed.; Lide, D. R., Ed.; CRC Press: Boca Raton, 2005; pp 4−7.
(29) Nishiwaki, N.; Konishi, T.; Hirao, S.; Yamashita, Y.; Yoshikawa, H.; Shimoda, M. Hydroxylated Surface of GaAs as a Scaffold for a Heterogeneous Pd Catalyst. *Phys. Chem. Chem. Phys.* **2012**, *14*, 1424−1430.
(30) Mani, R.; Mahadevan, V.; Srinivasan, M. Characterization of a Polymer-Bound Palladium Acetate Catalyst and Studies on the Selective Hydrogenation of Dienes and Alkynes. *J. Macromol. Sci., A* **1993**, *30*, 557−569.
(31) Jia, L. J.; Bulushev, D. A.; Beloshapkin, S.; Ross, J. R. H. Hydrogen Production from Formic Acid Vapour over a Pd/C Catalyst Promoted by Potassium Salts: Evidence for Participation of Buffer-Like Solution in the Pores of the Catalyst. *Appl. Catal., B* **2014**, *160−161*, 35−43.
(32) Kohiki, S.; Ikeda, S. Photoemission from Small Palladium Clusters Supported on Various Substrates. *Phys. Rev. B* **1986**, *34*, 3786−3797.
(33) Wu, T. P.; Kaden, W. E.; Kunkel, W. A.; Anderson, S. L. Size-Dependent Oxidation of Pd_n (N<13) on Alumina/NiAl (1 1 0): Correlation with Pd Core Level Binding Energy. *Surf. Sci.* **2009**, *603*, 2764−2770.
(34) Chen, L.; Yelon, A.; Sacher, E. X-ray Photoelectron Spectroscopic Studies of Pd Nanoparticles Deposited onto Highly Oriented Pyrolytic Graphite: Interfacial Interaction, Spectral Asymmetry, and Size Determination. *J. Phys. Chem. C* **2011**, *115*, 7896−7905.
(35) Pels, J. R.; Kapteijn, F.; Moulijn, J. A.; Zhu, Q.; Thomas, K. M. Evolution of Nitrogen Functionalities in Carbonaceous Materials During Pyrolysis. *Carbon* **1995**, *33*, 1641−1653.
(36) Simonov, P. A.; Romanenko, A. V.; Prosvirin, I. P.; Moroz, E. M.; Boronin, A. I.; Chuvilin, A. L.; Likholobov, V. A. On the Nature of the Interaction of H_2PdCl_4 with the Surface of Graphite-like Carbon Materials. *Carbon* **1997**, *35*, 73−82.
(37) Kondrat, S. A.; Shaw, G.; Freakley, S. J.; He, Q.; Hampton, J.; Edwards, J. K.; Miedziak, P. J.; Davies, T. E.; Carley, A. F.; Taylor, S. H.; Kielyb, K. J.; Hutchings, G. J. Physical Mixing of Metal Acetates: A Simple Scalable Method to Produce Active Chloride Free Bimetallic Catalysts. *Chem. Sci.* **2012**, *3*, 2965−2971.
(38) Santacesaria, E.; Cozzolino, M.; Balato, V.; Tesser, R.; di Serio, M.; Ruffo, F. Preparation and Characterisation of Dispersed Palladium Catalysts Supported on Carbon Previously Treated with Different Strong Oxidants. *Chem. Sustainable Dev.* **2006**, *14*, 605−611.
(39) Bulushev, D. A.; Yuranov, I.; Suvorova, E. I.; Buffat, P. A.; Kiwi-Minsker, L. Highly Dispersed Gold on Activated Carbon Fibers for Low-Temperature CO Oxidation. *J. Catal.* **2004**, *224*, 8−17.
(40) Hu, C. Q.; Pulleri, J. K.; Ting, S. W.; Chan, K. Y. Activity of Pd/C for Hydrogen Generation in Aqueous Formic Acid Solution. *Int. J. Hydrogen Energy* **2014**, *39*, 381−390.
(41) Gosselink, R. W.; Xia, W.; Muhler, M.; de Jong, K. P.; Bitter, J. H. Enhancing the Activity of Pd on Carbon Nanofibers for Deoxygenation of Amphiphilic Fatty Acid Molecules through Support Polarity. *ACS Catal.* **2013**, *3*, 2397−2402.
(42) Wang, Z.-L.; Yan, J.-M.; Ping, Y.; Wang, H.-L.; Zheng, W.-T.; Jiang, Q. An Efficient CoAuPd/C Catalyst for Hydrogen Generation from Formic Acid at Room Temperature. *Angew. Chem., Int. Ed.* **2013**, *52*, 4406−4409.
(43) Wang, Z. L.; Ping, Y.; Yan, J. M.; Wang, H. L.; Jiang, Q. Hydrogen Generation from Formic Acid Decomposition at Room Temperature Using a NiAuPd Alloy Nanocatalyst. *Int. J. Hydrogen Energy* **2014**, *39*, 4850−4856.
(44) Jia, L. J.; Bulushev, D. A.; Podyacheva, O. Y.; Boronin, A. I.; Kibis, L. S.; Gerasimov, E. Y.; Beloshapkin, S.; Seryak, I. A.; Ismagilov, Z. R.; Ross, J. R. H. Pt Nanoclusters Stabilized by N-Doped Carbon Nanofibers for Hydrogen Production from Formic Acid. *J. Catal.* **2013**, *307*, 94−102.
(45) Wang, Z. L.; Yan, J. M.; Wang, H. L.; Ping, Y.; Jiang, Q. Au@Pd Core-Shell Nanoclusters Growing on Nitrogen-Doped Mildly Reduced Graphene Oxide with Enhanced Catalytic Performance for Hydrogen Generation from Formic Acid. *J. Mater. Chem. A* **2013**, *1*, 12721−12725.
(46) Zacharska, M.; Podyacheva, O. Y.; Kibis, L. S.; Boronin, A. I.; Senkovskiy, B. V.; Gerasimov, E. Y.; Taran, O. P.; Ayusheev, A. B.; Parmon, V. N.; Leahy, J. J.; Bulushev, D. A. Ruthenium Clusters on Carbon Nanofibers for Formic Acid Decomposition: Effect of Nitrogen-Doping of the Support. *ChemCatChem* **2015**, DOI: 10.1002/cctc.201500216.

DOI: 10.1021/acsami.5b00983
ACS Appl. Mater. Interfaces 2015, 7, 8719−8726